HYBRID ROCKET COMBUSTION STUDY

H. D. Strand* and R. L. Ray
Jet Propulsion Laboratory
California Institute of Technology
Pasadena, California

N. S. Cohen*
Cohen Professional Services
Redlands, California

Abstract

The objectives of this study of "pure" or "classic" hybrids are to (1) extend our understanding of the boundary layer combustion process and the critical engineering parameters that define this process, (2) develop an up-to-date hybrid fuel combustion model, and (3) apply the model to correlate the regression rate and scaling properties of potential fuel candidates. Tests were carried out with a hybrid slab window motor, using several diagnostic techniques, over a range of motor pressure and oxidizer mass flux conditions. The results basically confirmed turbulent boundary layer heat and mass transfer as the rate limiting process for hybrid fuel decomposition and combustion. The measured fuel regression rates showed good agreement with the analytical model predictions. The results of model scaling calculations to Shuttle SRM size conditions are presented.

Nomenclature

A_f - Arrhenius prefactor for fuel binder decomposition

a_g constant in expression for gas emissivity

a_p - constant in expression for particle cloud emissivity

B - Spalding number

$$B = \frac{\bar{C}_g T'_g - C_s T'_s}{C_s (T'_s - T'_0) + \alpha_F Q_F + \alpha_{Al} Q_m} \qquad (1)$$

* Associate Fellow AIAA

c_g	specific heat of combustion gases
c_s	specific heat of solid fuel
f',	activation energy for fuel binder decomposition
G	mass flux (total) through fuel port
G_{ox}	oxidizer mass flux at head-end of fuel port
K	convective heating constant
l	radiation path length
N_p	particle number density
o/F	ratio of oxidizer/fuel mass flow rates
P	pressure
Pr	Prandtl number
QF	heat of decomposition of fuel binder
Q_m	heat of fusion of aluminum
R	universal gas constant
r	fuel regression rate
r_{moan}	time and spatially averaged fuel regression rate
T_g	gas temperature
T_o	initial fuel bulk temperature
T_p	radiating particle temperature
T_s	fuel surface temperature
x	distance from head-end of fuel grain
α_f	weight fraction of binder
α_{Al}	weight fraction of aluminum
ϕ_C	convective heat flux
$\phi_{R,g}$	radiative heat flux from gas
$\phi_{R,p}$	radiative heat flux from particle cloud

μ - gas viscosity

ρ_f - density of fuel binder

ρ_s - density of solid fuel

σ - Stefan-Boltzmann constant

Introduction

Hybrid rocket propulsion is of interest for advanced launch vehicle applications. It offers advantages of safety, lower cost, more benign combustion products, attractive performance, and mission flexibility relative to current rocket boosters.[1]

For the classical hybrid cycle (oxidizer injection into the forward end of an inert fuel grain) the combustion process occurs in a turbulent boundary layer diffusion flame. Extensive research in the 1960s[2-5] demonstrated that for non-metal containing fuels operating at normal pressures, >1.75 MPa (250 psia), and oxidizer flow rates, the mixing anti reaction of the vaporizing fuel grain with the oxidizer flowing over the grain and transfer of heat back to the fuel surface is the overall rate-limiting process. In other words, the fuel regression rate is controlled by the fluid dynamics of the turbulent boundary layer established on the solid fuel surface. Classical hybrid regression rates tend, therefore, to be low, <0.25 cm/s (0.1 in./s), and dependent on the fuel' grain geometry. "This has an impact on the volumetric loading and utilization efficiencies of the solid fuel.

10 aid in the development of large-scale rocket motors, a study was initiated with the objectives of extending our understanding of the nature of the boundary layer combustion process (fuel decomposition, heat and mass transfer, and chemical reaction) and the critical engineering parameters that define this process and to develop an up-to-date hybrid fuel combustion model, based on models developed in the 1960s[6], for guiding fuel developments, predicting regression rates in motors, and optimizing the design of hybrid rockets.

] est Program

1 he study is being carried out using a hybrid slab window motor system shown schematically in Figure 1. It consists of a (1) head-end closure, (2) flow straightener/ igniter section with (3) flow straightening screens, (4) test

JPL

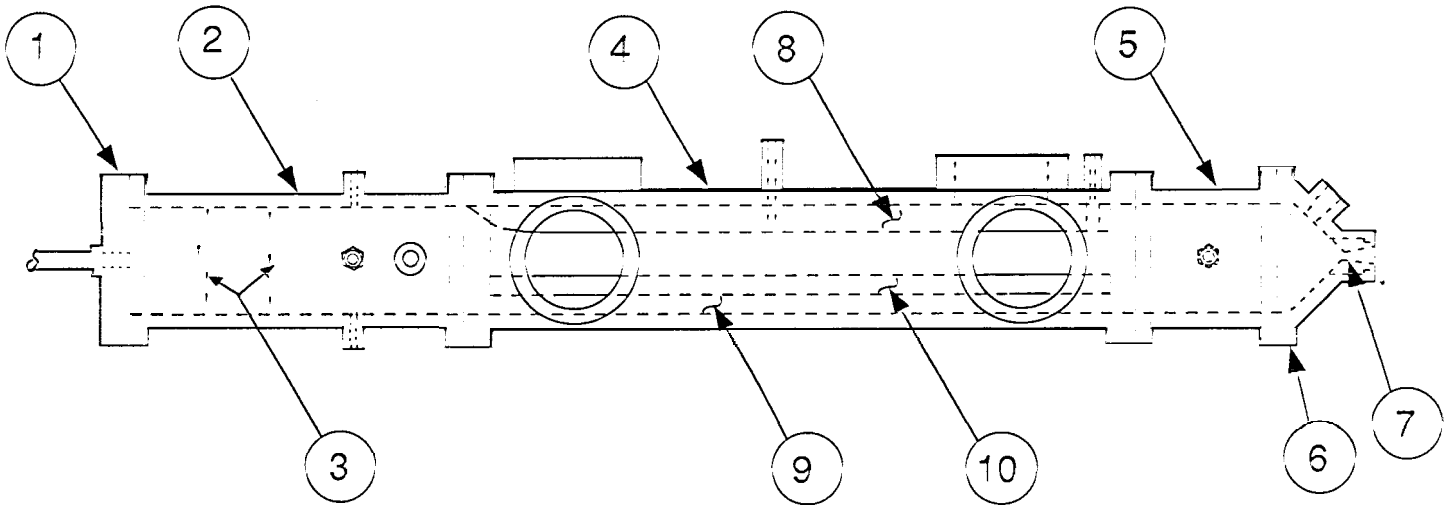

section with quartz viewing ports, (5) aft combustor section, (6) aft closure with (7) graphite nozzle, (8) internal spacer to control burner cross-sectional area, (9) fuel casting base plate, and (1 O) fuel slab. For a complete description of the system, the reader is referred to Ref. 7.

The fuel and oxidizer for this study are R-45M hydroxyl-terminated polybutadiene (H-I PB) and gaseous oxygen, respectively. 0.3% carbon is added to the HTPB to increase its radiation absorption coefficient. Tests were carried out over a pressure range of 1 to 2 MPa (140 - 280 psia) and head-end oxidizer mass flux (mass flow/port area) range of 0.7 to 7 gm/cm^2-s (0.01 - 0.1 lb_m/in^2-s). Besides measurement of burner mean pressure and temperature lower limit (tungsten-rhenium thermocouple), combustion behavior diagnostics consist of motion picture and high speed digital video (4000 images/s) coverage through the forward and aft viewing ports. The time-averaged fuel regression rates were determined by both before and after measurement and weighing of the fuel slabs.

A hot wire anemometer was inserted in one of the spark plug igniter ports, and the turbulence level of the gaseous oxygen (GOX) core flow into the motor test section was measured under cold flow conditions duplicating the actual test oxygen mass flows and chamber pressures.

Test Results

Fuel Regression Rate

-Mean!-c-orre!at! on

Figure ? shows r_{mean}, as calculated from before and after measurement of the fuel slabs, plotted versus time-averaged G_{ox}. The data points are separated into the two indicated chamber pressure ranges. A power law curve fit yielded an exponent of unity. Plotted in this manner, the exponent is a function of the motor configuration, As will be shown later, plotting r_{mean} versus the total mass flux resulted in the near-0.8 power law dependence predicted by turbulent boundary layer diffusion flame theory. Figure 3 shows the results as calculated from before and after weighing of the fuel slabs, The regression rate was observed to be independent of pressure over the G_{ox} range tested. For the lower test-pressure range at least, the dependence on G_{ox} diminishes at the upper test values. 1 his indicates that

Fig 2 MEAN REGRESSION RATE VS OXYGEN MASS FLUX

MEASUREMENT RESULTS

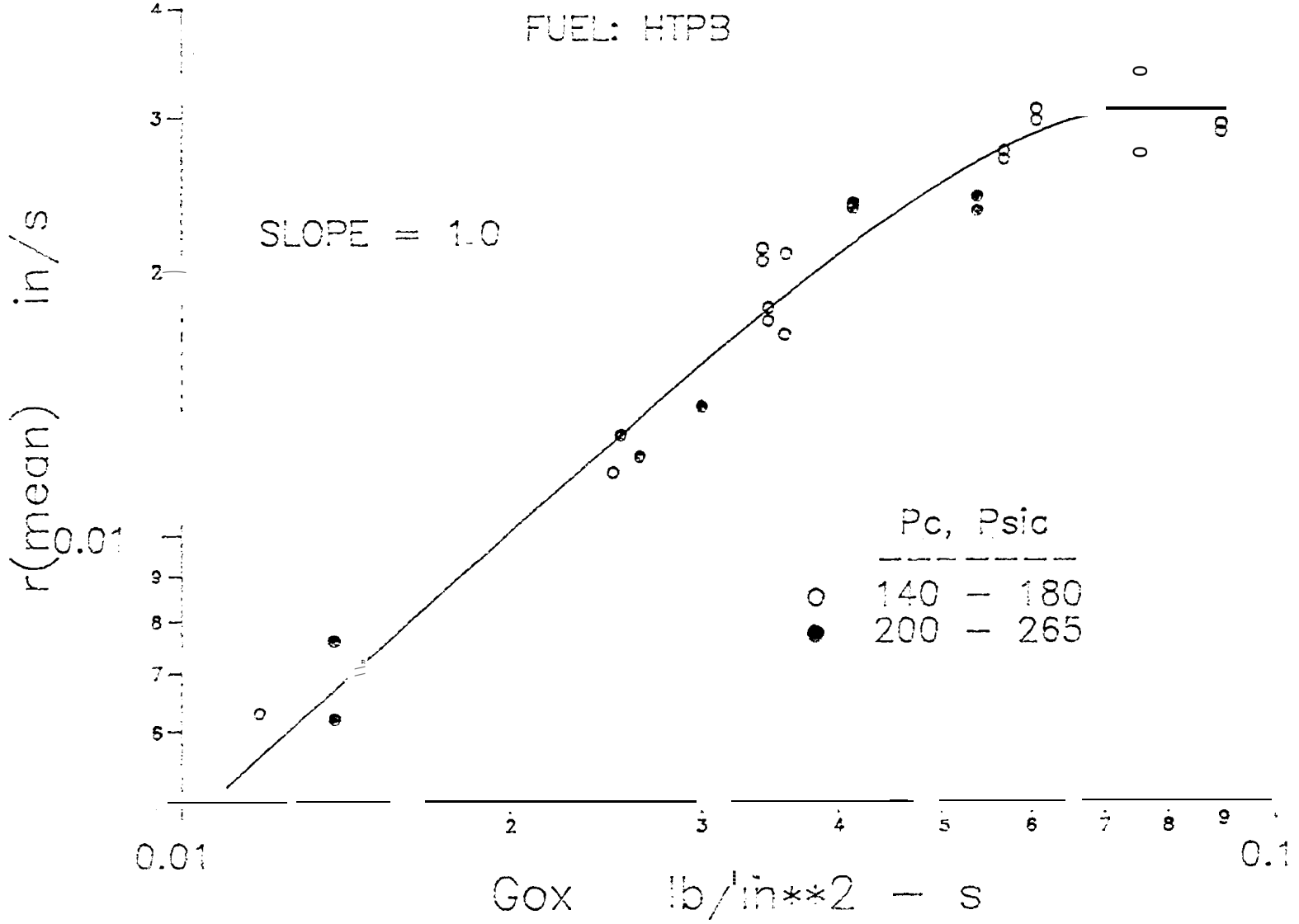

Fig 3

MEAN REGRESSION RATE VS OXYGEN MASS FLUX

WEIGHT RESULTS

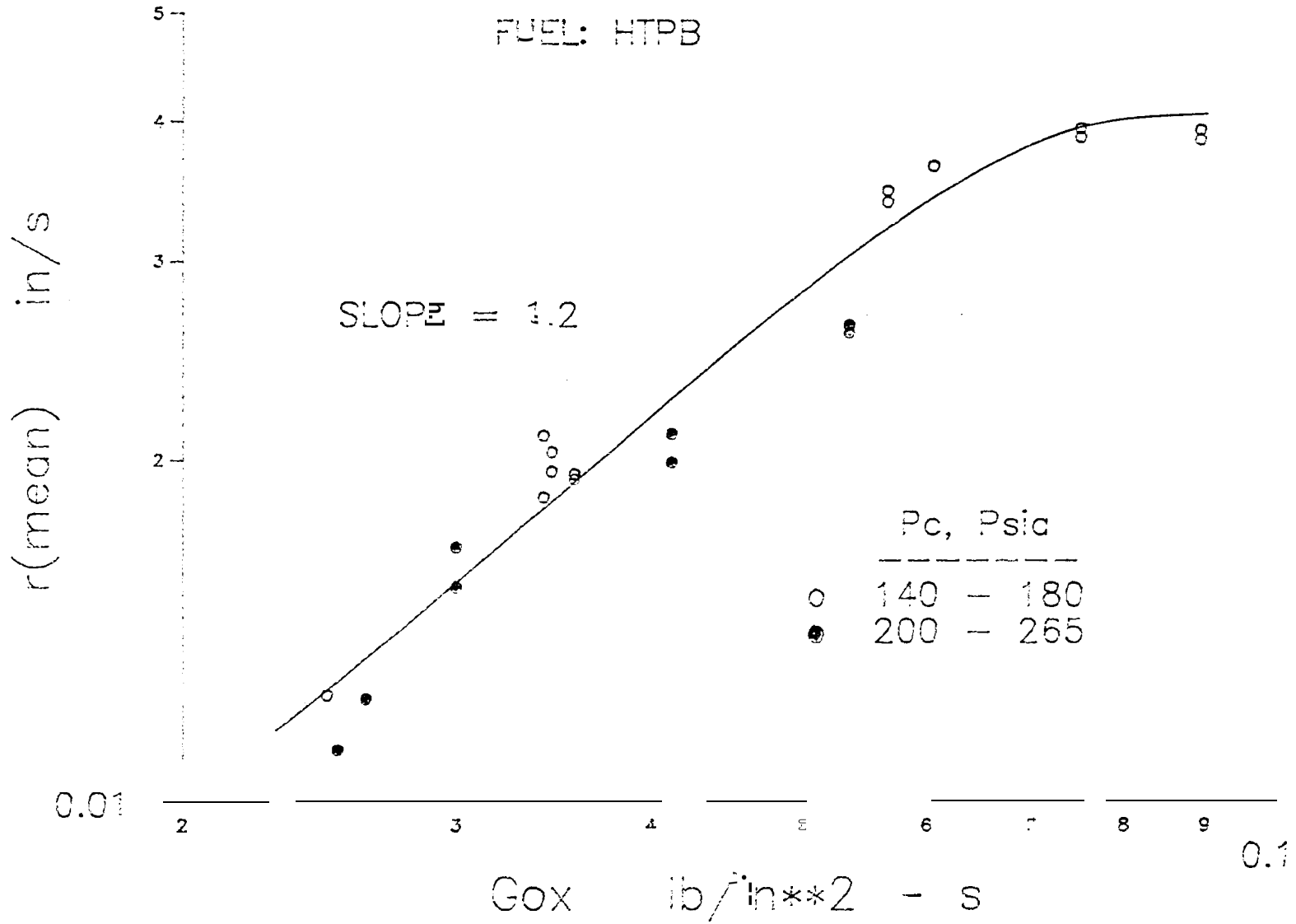

another process, probably the flame chemical kinetics, is becoming rate-limiting.[8] This will be discussed further in the analytical model section,

Spatial Dependence

Figures 4 and 5 show the initial and post-test average thickness versus axial position profiles for two fuel slabs that were each used in five test firings, 1 he respective test mean G_{ox} values are indicated, At these G_{ox} levels the results show little variation in regression with axial position, except at the 1 /4length position, From the high speed video results and the hollowed out, surface melt nature of the quenched surface, this augmented regression appears to be due to turbulent mixing enhancement resulting from vortices shed from the slab forward face.

Turbulence Magnitude

Figure 6, a portion of the achot wire anemometer trace for a cold flow test at a G_{ox} of 6.4 gm/cm^2-s (0.09 lb/in^2-s) and motor chamber pressure of 1.9 Mf'a (275 psia), shows typical results. The amplitude of the oscillations is approximately 10% of the flow mean velocity. Analysis of the spectral density power showedbroad-band content decreasing logarithmically with frequency. 1 his broad-band content should also be characteristic of the corresponding hot-flow test condition.

Irregular Combustion

1 he pressure traces for most tests exhibited low-frequency, sub-acoustic pressure oscillations in varying degrees of strength. Figure 7 depicts the largest amplitudes observed to date. These bulk-mode oscillations are believed to be a motor chamber mass filling-venting phenomenon similar to solid rocket L*-instability.For the test conditions depicted in Figure 7, an approximate L*-instability calculation, adapting the theory of Beckstead and Price[9], predicted a pressure oscillation frequency of 3 to 4 Hz.

As to the source of this irregular combustion, tests reported elsewhere[10] indicate that it is not due to the oxygen feed, or turbulence induced by the step at the aft end of the slabs, or the combustion of the mixture in the aft-combustor volume. I-he remaining, actual driving mechanism is speculated to be some type of flow-combustion turbulence interaction along the surface of the fuel slab,

Fig. – POST-TEST FUEL SLAB THICK-NESS vs AXIAL DISTANCE

BATCH/CHARGE NO.: LS 126/101

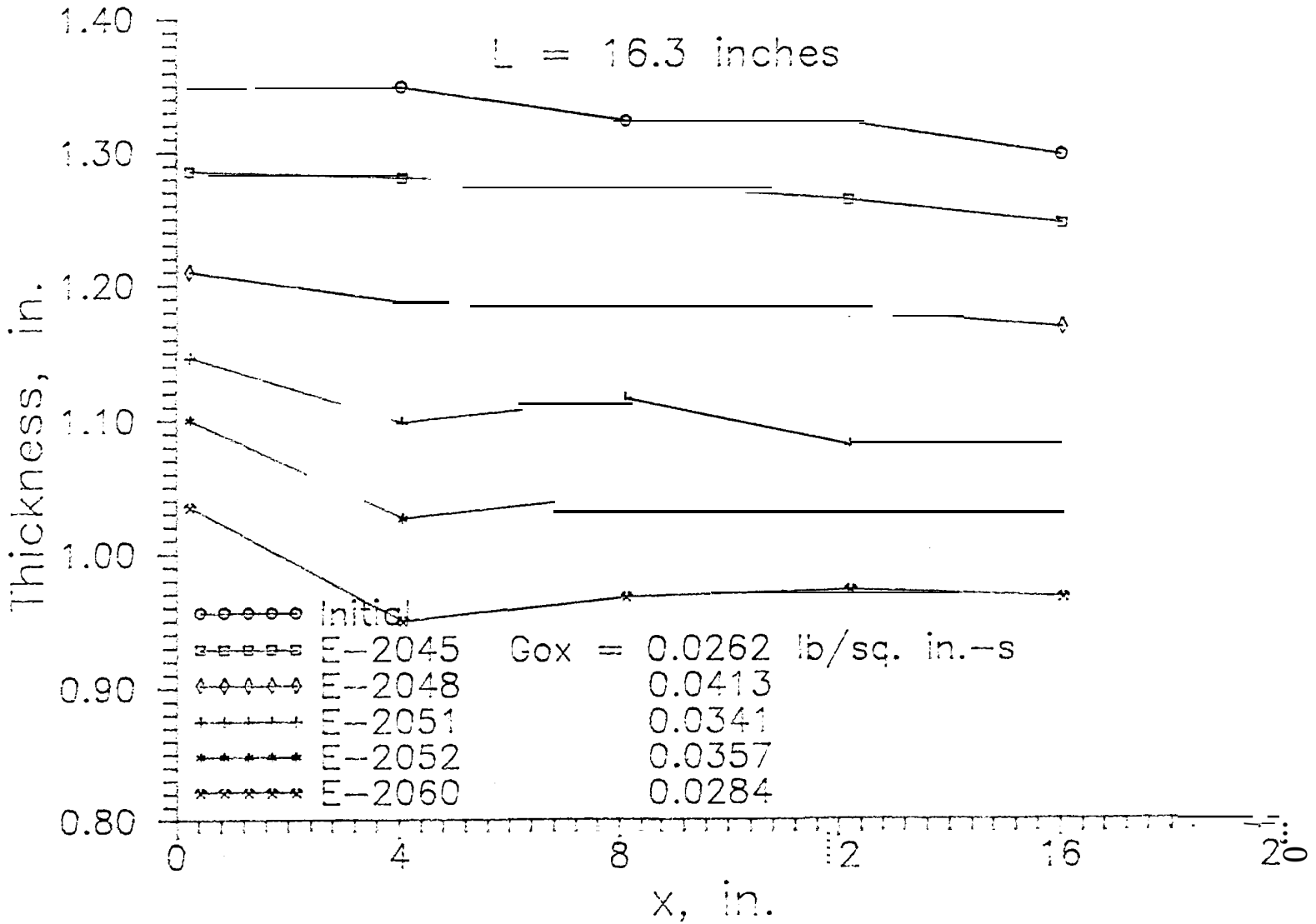

Fig. 5

POST-TEST FUEL SLAB THICKNESS vs AXIAL DISTANCE

BATCH/CHARGE NO.: LS 12B/102

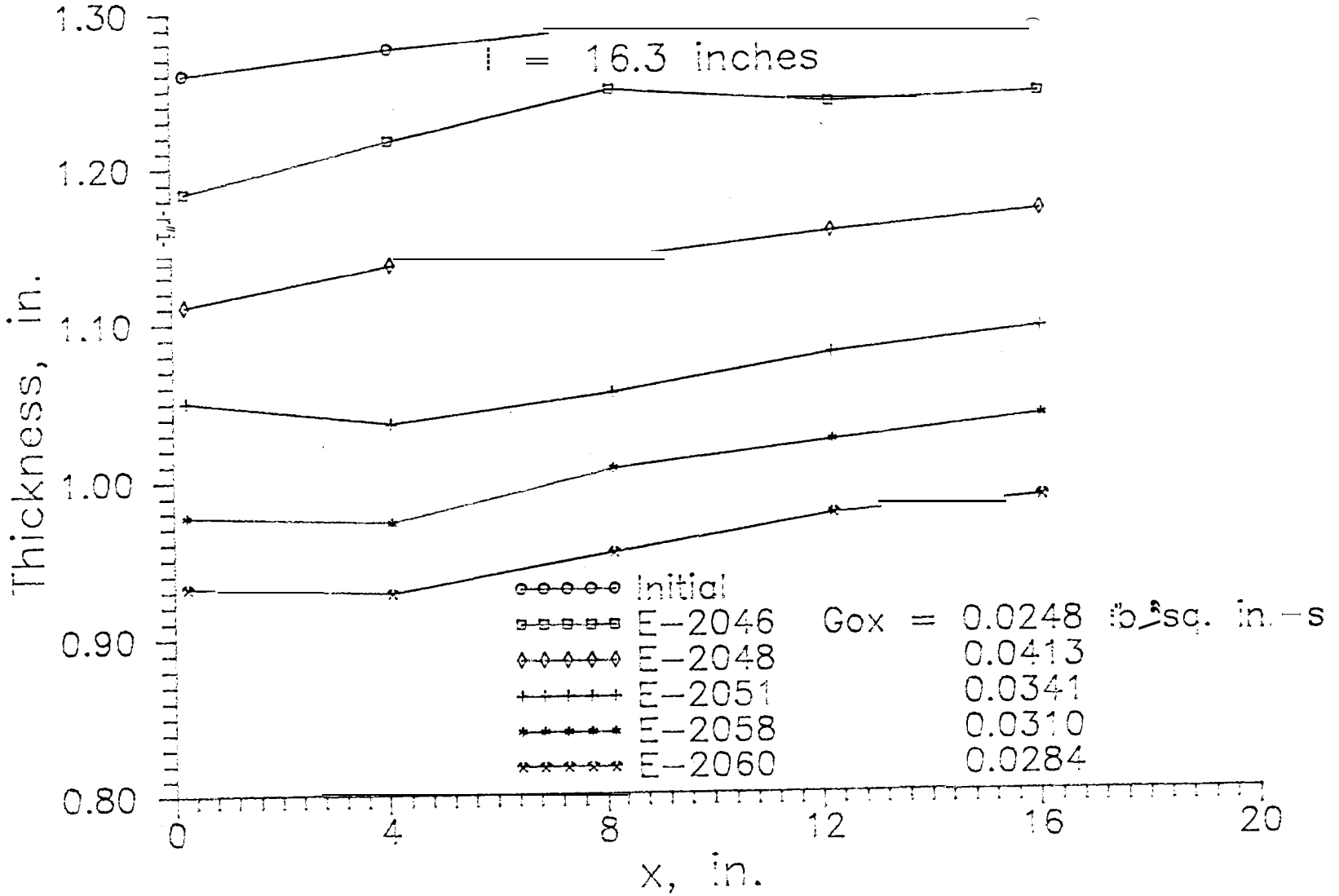

JET PROPULSION LABORATORY
HYBRID COLD-FLOW TEST
RUN E-2065 TURBULENCE MAGNITUDE

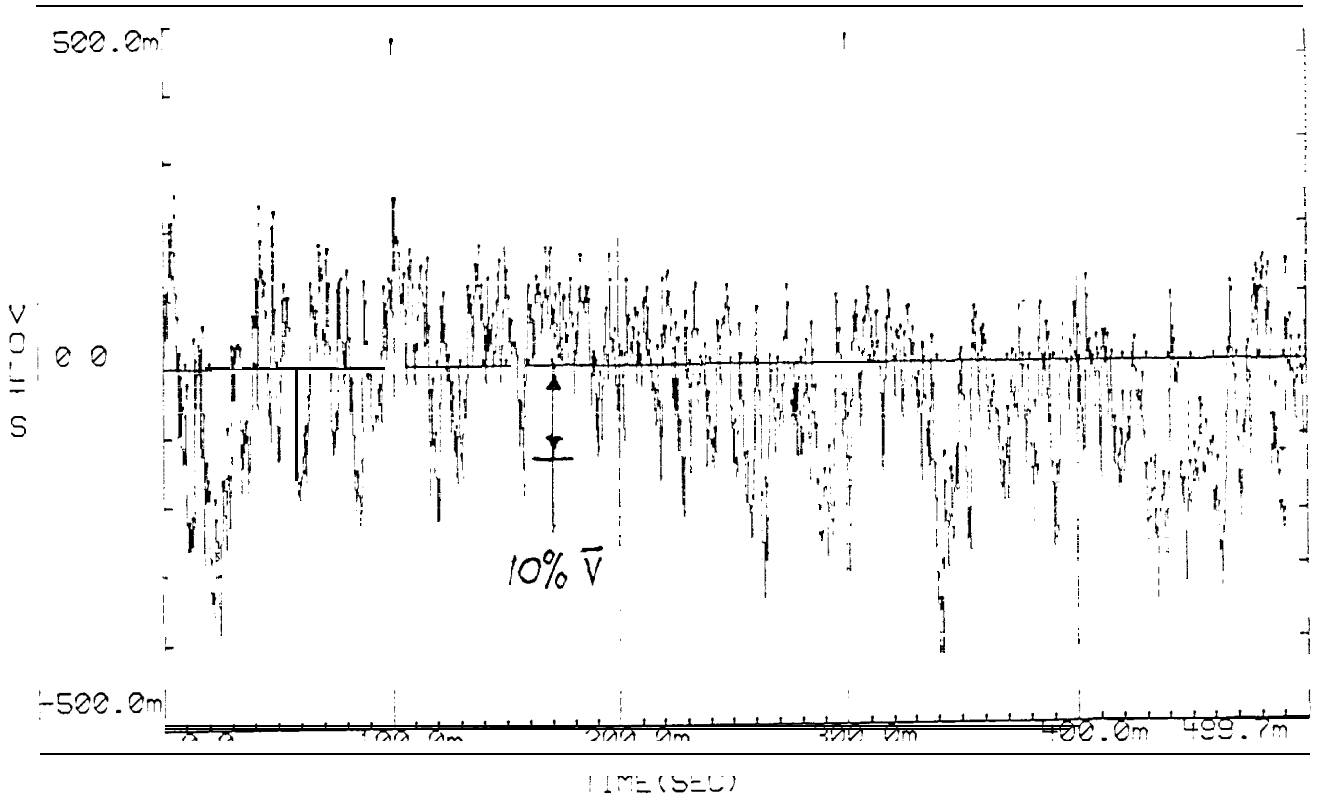

Fig. 6 Cold-flow measurements of GOX head end turbulence magnitude.

Fig. 7 Worst case example of irregular combustion.

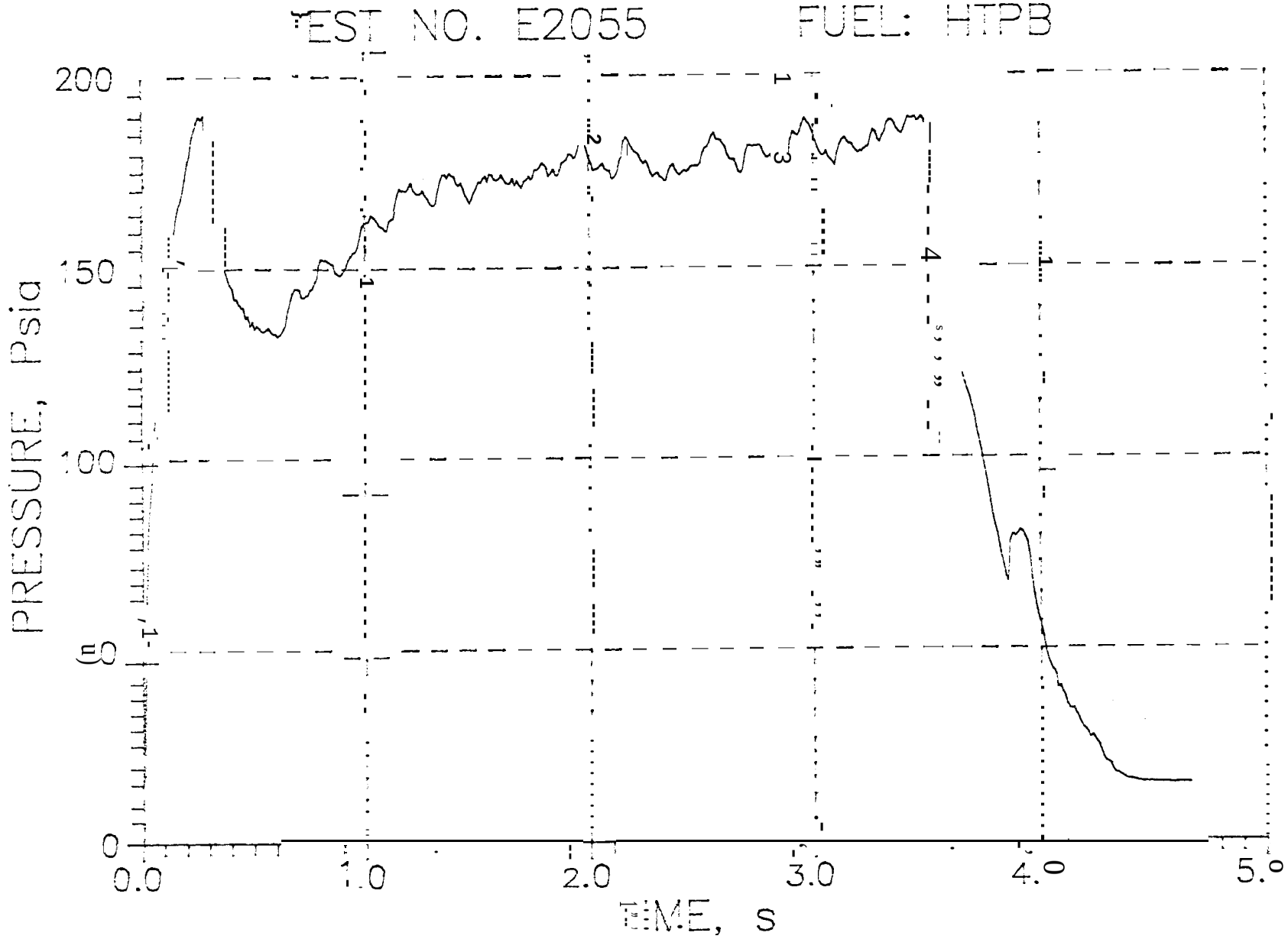

Analytical Combustion Model

Analysis of the Condensed Phase

The models of the 1960s[6] lacked an adequate description of the condensed phase. The energy balance was lumped into an empirical parameter, the kinetics of fuel decomposition was not considered, and the surface temperature of the fuel was an assumed input quantity. Current knowledge enables these deficiencies to be remedied.

The energy balance at the fuel surface for a metal (Al) containing fuel can be written as:

$$\rho_s r \left[c_s (T_s - T_o) + \alpha_F Q_F + \alpha_{Al} Q_m \right] = \Phi_C + \Phi_R \qquad (1)$$

The regression rate of the polymer is governed by Arrhenius kinetics:

$$\rho_F r = A_F \exp\left(-\frac{E_F}{R T_s} \right) \qquad (2)$$

Kinetics constants, thermal properties, and heats of decomposition have been measured for a variety of polymers of interest.[11]

Analysis of the Gas Phase

The regression rate of the fuel is driven by heat transfer from the combustion zone in the gas phase. It is well-settled that there are two primary modes of heat transfer under the conditions of practical interest. First, convective transport from the turbulent boundary layer diffusion flame as modified by the surface transpiration (blowing) of the fuel binder, Second is radiation from the gases (and particulate clouds for metal containing fuels) that fill the fuel port cavities, It has been established that radiation is the primary mechanism for the pressure dependence of fuel regression rate under pressure conditions of practical interest.[6] Reaction kinetics do not contribute to a pressure dependence under these conditions because they are much faster than the rate-limiting diffusion process. Absent radiation, regression rates are dependent upon local mass flux and length position in accordance with turbulent convective transport theory.

1 he gas phase model of Smoot and Price[3] was cast into the following expression to describe the convective heating component of the energy balance equation:

$$\phi_C = \{C_g(T'_s - T'_0) \quad \alpha_F Q_F + \alpha_{Al} Q_m\}$$

$$\{KG^{0.8}\left(\frac{\mu}{x}\right)^{0.2} \ln\left(+ \frac{\alpha_F B}{Pr^{2/3}}\right) \quad (3)$$

Radiation components are expressed as:

$$\phi_{R,g} = \sigma T_g^4(1 - e^{-a_g PL}) \quad (4)$$

$$\phi_{R,p} = \sigma T_p^4(1 - e^{-a_p N_p}) \quad (5)$$

Radiation measurements for the combustion products of the test propellant systems are in preparation. In the absence of {measurements, the following assumptions were made to determine the emissivities. For the gases, data reported for a high energy non-aluminized solid propellant formulation[12] were used to obtain values for a_g. It turned out that radiation from the gases was negligible in the slab combustor tests, as confirmed by the absence of that type of pressure effect in Figures 2 and 3. For the aluminum particle cloud it was assumed that all the aluminum burned efficiently to fine aluminum oxide smoke, and data from solid propellant exhaust plumes[13, 14] were used to quantify a_p. Combining this with an expression for the number density of the oxide smoke particles, the result was:

$$a_p N_p = 0.00141 \frac{\alpha_{Al} P}{\alpha_F + O/F} \quad (6)$$

This radiation component was significant in previous slab motor tests carried out with a heavily aluminized (40% by weight) HTPB fuel, confirmed by the pressure dependence of the regression rates.[7]

Discussion

The foregoing equations can be combined to iterate for regression rate and surface temperature. They are of a form that has been used in the past to correlate and scale hybrid fuel regression rate data.[6, 15] They are also instructive. For example, regression rates can be increased by using a binder having a low heat of decomposition and by filling it with a significant fraction of particulate that would provide strong radiation components. Moreover, the greater the influence of the particulate, the less the regression rate will depend upon the local mass flux.

Model Calculations

HTPB Fuel

Figure 8 presents the fit to the HTPB fuel regression rate data, plotted here versus the time- and spatially-averaged total mass flux, together with results of model calculations. To give this work some perspective, past data for other fuels are included.

The data show the classical near-0.8 power law dependence of fuel regression rate on mass flux. Data for conditions leading to a kinetics pressure dependence (high mass flux, low pressure) were omitted. The model is observed to be in very good agreement with the data for the HTPB binder fuel,

The effect of the fuel composition on regression rate is interesting. From plexiglass to HTPB there is a factor of 3 increase in regression rate. Understanding the reason for this difference could be useful to the development of improved fuels. Unfortunately, relevant data for plexiglass in the context of this model were not available. However, data for Butarez are available to help explain the lower regression of the butyl rubber fuel compared to the HTPB of this work. Butarez has a higher specific heat, higher heat of decomposition, and slower decomposition kinetics than HTPB. These tend to lower regression rate. Other factors may have been present, such as a lower flame temperature under the conditions of the butyl rubber tests. These changes in binder properties were input into the model and the results are included in Figure 8. It is observed that the model can explain most, but not all, of the difference in the regression rate between butyl rubber and HTPB.

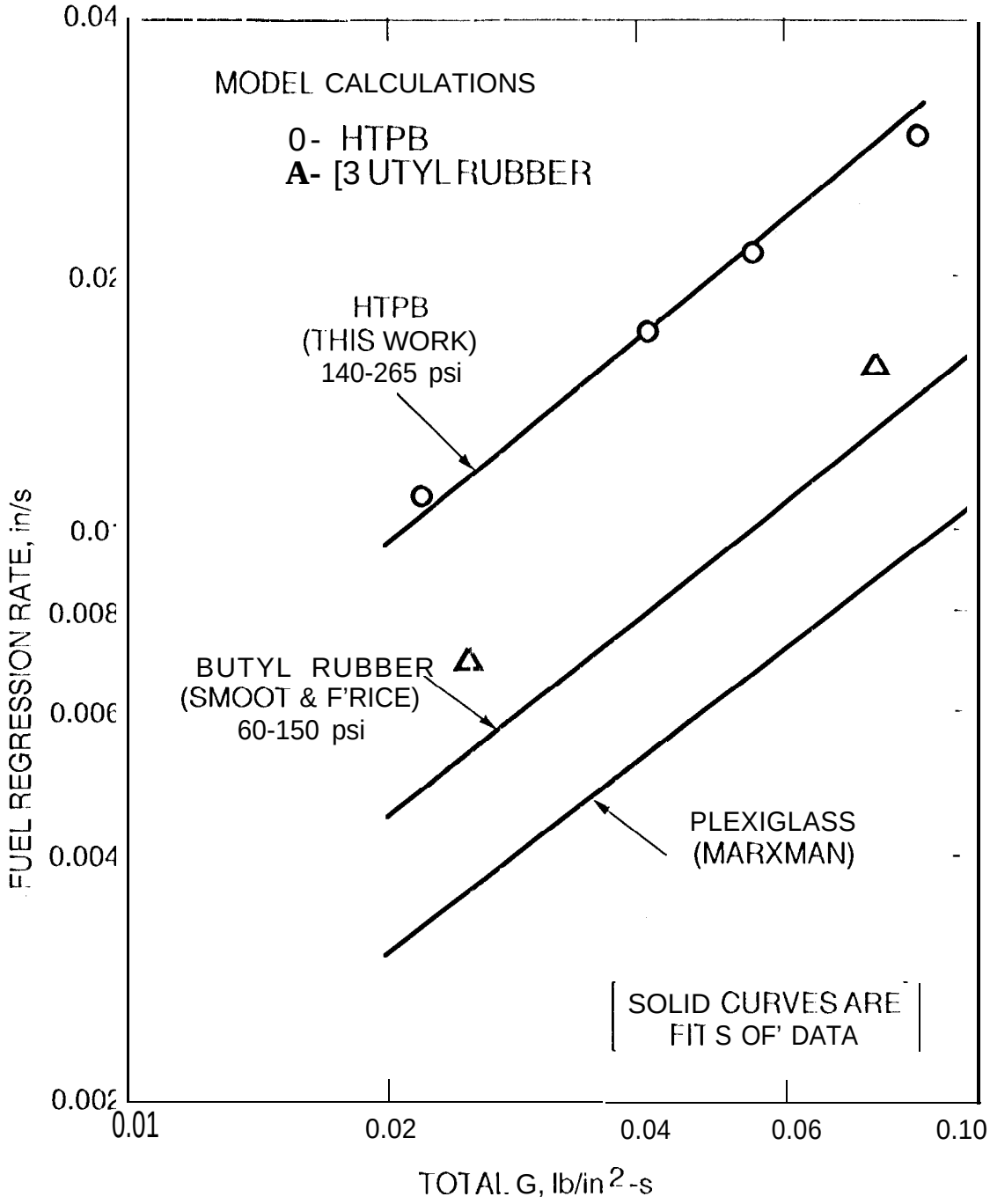

Fig. 8 Regression rates of non-metalized fuels, and results of model calculations (GOX injection).

Metallized HTPB Fuel

Figure 9 presents fits to the metallized (40% Al, 30% coal, 30% HTPB) hybrid fuel regression rate data' together with results of model calculations. These fillers increase the density of the fuel from 0.922 (HTPB alone) to 1,64 gm/cc, reduce the specific heat from 0.434 to 0.299 cal/gm-°K, and reduce the effective heat of decomposition of the fuel from 433 to 166 cal/gm. The dashed line extending the lower data curve is merely to illustrate the appearance of a classical 0.8 power law dependence, and is neither data nor a model result. Compared to the dashed line, the data fits and model results show a dependence that is less than 0.8. I-his is due to the effect of radiation, which becomes a stronger heat transfer contributor at lower values of G.

In modeling the coal filler it was assumed that the coal burned efficiently, such that it lost its particulate character and became part of the gas composition.

The model is observed to be in very good agreement with the higher pressure data, but overpredicts the regression rates at the lower pressure condition. 1 hus the pressure-sensitivity is greater in the data than predicted by the model. A possible explanation is an effect of pressure on aluminum combustion efficiency. At the lower pressure, a less efficient aluminum combustion would produce a lower number density of oxide smoke and therefore a reduced radiation component. At present, there is no basis for distinguishing larger unburned aluminum particles from the oxide smoke in the analysis.

The model predicts a reduced pressure sensitivity with increasing G, which is the expected result. This would also be shown by the data if the lower pressure data would more or less follow the dashed line extrapolation. However, it is possible that this higher exponent behavior would be followed because of improved aluminum combustion with increasing G, and not merely because of the growing dominance of convective heat transfer. Thus the model can be useful for data interpretation.

Scaling Calculations

Figure 10 represents the results of model calculations for the two fuels as scaled to Shuttle SRM booster conditions, together with the model results under the slab corn bustor conditions of lower pressure and lower G. The Shuttle SRM starts out at a pressure of 6.3 MPa (900 psi) at its initial web, and then provides a generally declining pressure with web burned to a final pressure of 2.8 MPa

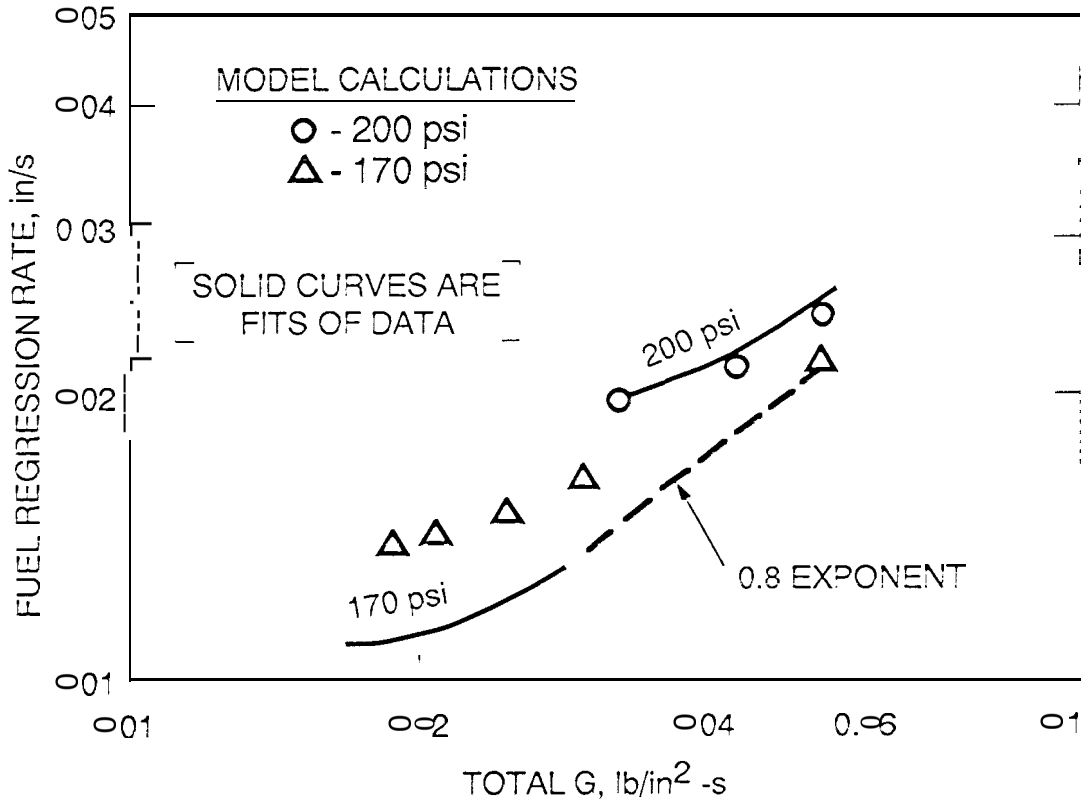

Fig. 9 Comparison of model calculations and data for metallized HTPB fuel (GOX injection).

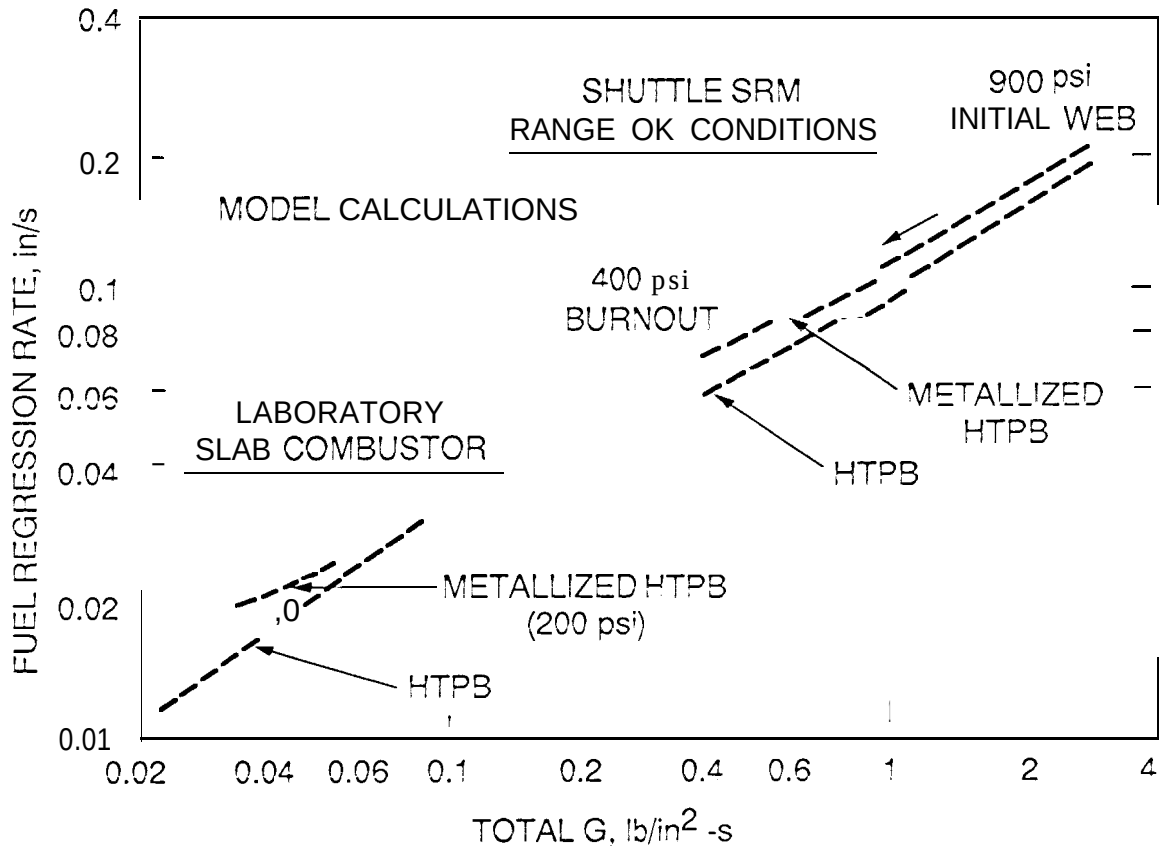

Fig. 10 Predicted scaling of HTPB fuels to SRM conditions.

(400 psi) near burn-out. The arrow on the figure denotes this path of operation. Note that the G range of operation is nearly two orders of magnitude greater, and that pressure is more than doubled, relative to the slab combustor. The scaled regression rates computed are values at the motor mid-length; this length scales to an amount comparable to the spatially averaged G.

It is predicted that radiation is significant in the SRM size, even for the unmetallized fuel, because of the greater path length as well as the higher pressures. Thus the G-dependence (slopes) of the two fuels are comparable in the SRM size, and are more like 0.6 than 0.8. This shows that radiation can still be effective at very high values of G if it is strong enough. The metallized fuel is predicted to burn faster because of its stronger radiation and lower enthalpy of decomposition.

Conclusions

The HTPB fuel results from this study (fuel regression rate dependence on G and non-dependence on P) confirm turbulent boundary layer heat and mass transfer as the rate limiting process for hybrid fuel decomposition and combustion under pressure conditions of practical interest. The nature of the fuel surface decomposition is altered (from dry to a surface melt) and the rate of regression is enhanced by augmentation of the boundary layer turbulent mixing. The observed weak dependence of fuel rate of regression on motor axial position also supports classical theory.

As a boundary condition for future fluid dynamic analysis of the slab motor, the amplitude of the GOX inlet core-flow turbulence was approximately 10% of the mean velocity in cold-flow simulation tests.

The driving mechanisms for the bulk-mode pressure oscillations observed in these tests is speculated to be some type of flow-combustion turbulence interaction along the surface of the fuel slab,

An analytical model has been developed and applied to explain the regression rate behavior of non-metallized and metallized HTPB fuels. Future slab combustor experiments will employ heat transfer sensors to sort out and correlate convective and radiative heating components for hybrid combustion products.

Model calculations with the test propellants were scaled to Shuttle SRM booster conditions. The scaled fuel regression rates are still lower than SRM solid propellant burn rates and too dependent on geometry. However, desired regression rate properties appear to be within reach, and continued fuel developments should enable more efficient motor designs to be achieved.

Acknowledgments

The assistance of the Technical Operations personnel of the JPL Edwards Facility in performing the slab combustor experiments is gratefully acknowledged.

The research described in this paper was carried out at the Jet Propulsion Laboratory, California Institute of Technology, under contract with the National Aeronautics and Space Administration.

References

1. "What is the Future of Hybrid Rocket Propulsion for U.S. Space Launch Systems?", Position Paper by the National Space Propulsion Synergy Group, publication pending.

2. Marxman, G. A., Woolridge, C. E., and Muzzy, R. J., "Fundamentals of Hybrid Boundary Layer Combustion," Paper No. AIAA 63-505, Dec. 1963,

3. Smoot, L. D. and Price, C.F., "Regression Rate Mechanisms of Nonmetallized Hybrid Fuel Systems," AIAA J., Vol. 3, Aug. 1965, pp. 1408-1413.

4. Woolridge, C.E. and Muzzy, R. J., "Internal Ballistic Considerations in Hybrid Rocket Design," Paper No. AIAA 66-628, June 1966.

5. Marxman, G. A., "Boundary 1 ayer Combustion in Propulsionf" Eleventh Symposium (International) on Combustion, The Combustion Institute, Pittsburgh, PA, 1967.

6. Netzer, D. W., "Hybrid Rocket Internal Ballistics," CPIA Publication No. 222, Naval Postgraduate School, Monterey, CA, Jan, 1972.

7. Strand, 1.., Ray, R., Anderson, F., and Cohen, N., "Hybrid Rocket Fuel Combustion and Regression Rate Study", Paper No. AIAA 92-3302, AIAA/SAE/ASME/ASEE. 28th Joint Propulsion Conference, Nashville, TN, July, 1992.

8. Smoot, L.D. and Price, C. F., "Pressure Dependence of Hybrid Fuel Regression Rates, " AIAA J., Vol. 5, Jan. 1987, pp. 102-106.

9. Beckstead, M. W. and Price, E. W., "Nonacoustic combustion Instability, " AIAA J., Vol.5, Nov. 1967, pp. 1989-1996.

10. Cohen, N.S. and Strand, 1. D., "Hybrid Propulsion Based on Fluid-Controlled Solid Gas Generators, " Paper No. AIAA 93-2550, AIAA/SAE/ASME/ASEE 29th Joint Propulsion Conference, Monterey, CA, June 1993.

11. Cohen, N. S., Fleming, R.W., and Derr, R. 1.., "Role of Binders in Solid Propellant Combustion," AIAA J., Vol. 12, Feb. 1974, pp. 212-218.

12. Cohen, N. S., "Ballistic Predictions for Mass-Augmented Solid Rocket Motors, " Report AFRPL-TR-71-113, Lockheed Propulsion Co., Redlands, CA, Dec. 1971.

13. Kurtovich, D. D. and Pinson, G. T., "Radiation From an Aluminized Solid Propellant Rocket Engine, " Boeing Airplane Co., Aerospace Division, Seattle, WA, Jan. 1960.

14. McGrath, D. K., private communications, Thiokol Corporation, Elkton Division, Elkton, MD, 1988.

15. Estey, F'., Altman, D., and McFarlane, J., "An Evaluation of Scaling Effects for Hybrid Rocket Motors, " Paper No. AIAA-91-2517, AIAA/SAE/ASME 27th Joint Propulsion Conference, Sacramento, CA, June 1991.